ResearchGate

See discussions, stats, and author profiles for this publication at: https://www.researchgate.net/publication/37807675

Incremental Variation in the Number of Carbon Nanotube Walls with Growth Temperature

ARTICLE *in* THE JOURNAL OF PHYSICAL CHEMISTRY C · FEBRUARY 2009

Impact Factor: 4.77 · DOI: 10.1021/jp808316p · Source: OAI

CITATIONS
21

READS
40

6 AUTHORS, INCLUDING:

Prasantha R. Mudimela
King Abdullah University of Science and Te…
20 PUBLICATIONS **286** CITATIONS
SEE PROFILE

Albert G Nasibulin
Skolkovo Institute of Science and Technol…
234 PUBLICATIONS **3,853** CITATIONS
SEE PROFILE

Hua Jiang
Nanjing University of Science and Technol…
132 PUBLICATIONS **3,256** CITATIONS
SEE PROFILE

Toma Susi
University of Vienna
34 PUBLICATIONS **244** CITATIONS
SEE PROFILE

Available from: Toma Susi
Retrieved on: 01 February 2016

THE JOURNAL OF PHYSICAL CHEMISTRY C

Subscriber access provided by HELSINKI UNIV OF TECH

Article

Incremental Variation in the Number of Carbon Nanotube Walls with Growth Temperature

Prasantha R. Mudimela, Albert G. Nasibulin, Hua Jiang, Toma Susi, Delphine Chassaing, and Esko I. Kauppinen

J. Phys. Chem. C, **2009**, 113 (6), 2212-2218• DOI: 10.1021/jp808316p • Publication Date (Web): 15 January 2009

Downloaded from http://pubs.acs.org on March 20, 2009

More About This Article

Additional resources and features associated with this article are available within the HTML version:

- Supporting Information
- Access to high resolution figures
- Links to articles and content related to this article
- Copyright permission to reproduce figures and/or text from this article

View the Full Text HTML

ACS Publications
High quality. High impact.

The Journal of Physical Chemistry C is published by the American Chemical Society. 1155 Sixteenth Street N.W., Washington, DC 20036

ARTICLES

Incremental Variation in the Number of Carbon Nanotube Walls with Growth Temperature

Prasantha R. Mudimela,[†] Albert G. Nasibulin,*[,†] Hua Jiang,[†] Toma Susi,[†] Delphine Chassaing,[†] and Esko I. Kauppinen*[,†,‡]

Department of Engineering Physics and Center for New Materials, Helsinki University of Technology, P.O. Box 5100, Puumiehenkuja 2, FIN-02150 Espoo, Finland, and VTT Biotechnology, P.O. Box 1000, FIN-02044 VTT, Espoo, Finland

Received: June 1, 2008; Revised Manuscript Received: December 7, 2008

Investigations of carbon nanotube (CNT) synthesis were carried out in a chemical vapor deposition reactor using CO as the carbon source, Fe as the catalyst material, and SiO_2 as the catalyst support. This allowed us to synthesize CNTs in a wide range of diameters from 1.4 to 12 nm and lengths from 0.5 to 350 μm. An incremental variation in the number of CNT walls, increasing from one to four, was found in the temperature range of 590−1070 °C. The increase in CNT wall number and CNT length with temperature can be explained by enhancement of carbon solubility and diffusivity. CO_2 was found to be a very important additive for the activation of catalyst particles and subsequently for the successful synthesis of CNTs. The prevention of cementite particle formation and etching amorphous carbon were also attributed to CO_2.

1. Introduction

Carbon nanotubes (CNTs) are the basic building blocks in nanoscience and nanotechnology. They attracted significant interest instantly following Iijima's landmark publication[1] and still hold the attention of the scientific community because of their extraordinary physical and chemical properties.[2,3] Several applications have been demonstrated for this material.[4−8] However, success in any application strongly depends on the ability to synthesize defect-free nanotubes with controlled diameter, length, and wall structure.

The known techniques for CNT fabrication can be divided into two types, physical and chemical, according to the carbon atomization method. The physical method is usually based on the local application of high energy to a graphite target resulting in the evaporation of carbon.[9−11] The chemical method of CNT synthesis utilizes disintegration of carbon-containing precursor materials on the surface of catalyst, which can be suspended in a gas phase as an aerosol (floating catalyst)[12−14] or supported on a substrate.[15−17] The obvious advantage of the chemical method (chemical vapor deposition, CVD) is the possibility of producing CNTs at controlled conditions and at relatively low temperatures. Existing synthesis techniques allow for producing certain types of CNTs: mulitwalled CNTs, few-, double-, and single-walled CNTs, and their mixtures.[18−21] In spite of much progress in CNT syntheses,[22−25] the possibility of producing CNTs with a controlled and an adjusted number of walls is still a challenging task. Each type of CNT is of specific interest, e.g., single-walled CNTs are super strong, metallic or semiconductive, chemically inert and possess many other useful properties. Double-walled and thin multiwalled CNTs are, in addition to the advantages of the single-walled CNTs, more robust and can be structurally and electronically modified by functionalization, with intact inner tubes;[26] therefore, they might possess new properties and potential applications differing from those of other types of CNTs.[27] In addition, control of the wall number could help in adjusting the electronic properties of individual CNTs and networks of CNTs because increasing the number of walls results in an increase in the CNT metallicity.

Here, we report the opportunity of tuning the number of CNT walls in the CVD synthesis method. We show that the number of walls could be altered from one to four by changing the gas composition and the processing temperature from 590 to 1120 °C. As a carbon source we used CO, which is known to produce quite clean CNTs,[15,28,29] in sense of amorphous carbon because of the solely catalytic CO disproportionation behavior. Conditions of nanotube growth were examined on the basis of systematic investigations, FT-IR measurements of the gaseous products, and thermodynamic calculations.

2. Experimental Section

2.1. Description of Experimental Setup. CNT synthesis was carried out in a vertical laminar flow reactor consisting of a ceramic tube with an inner diameter of 2.2 cm placed inside a 44-cm-long furnace (Figure 1). Thermally oxidized (300 nm thickness) silicon wafers were used as a substrate. Iron utilized as the catalyst was sputtered on the silica wafer using an Agar sputter coater (model 108A) under 0.05 mbar Ar pressure at 20 mA DC. In our experiments sputtering time was varied from 5 to 20 s.

For CNT growth, the reactor was first heated to the desired temperature in an Ar flowing atmosphere (400 cm^3/min). A piece of a silica wafer (about 1 cm × 1 cm) with deposited catalyst

* To whom correspondence should be addressed. E-mail: albert.nasibulin@hut.fi, esko.kauppinen@hut.fi.
† Helsinki University of Technology.
‡ VTT Biotechnology.

10.1021/jp808316p CCC: $40.75 © 2009 American Chemical Society
Published on Web 01/15/2009

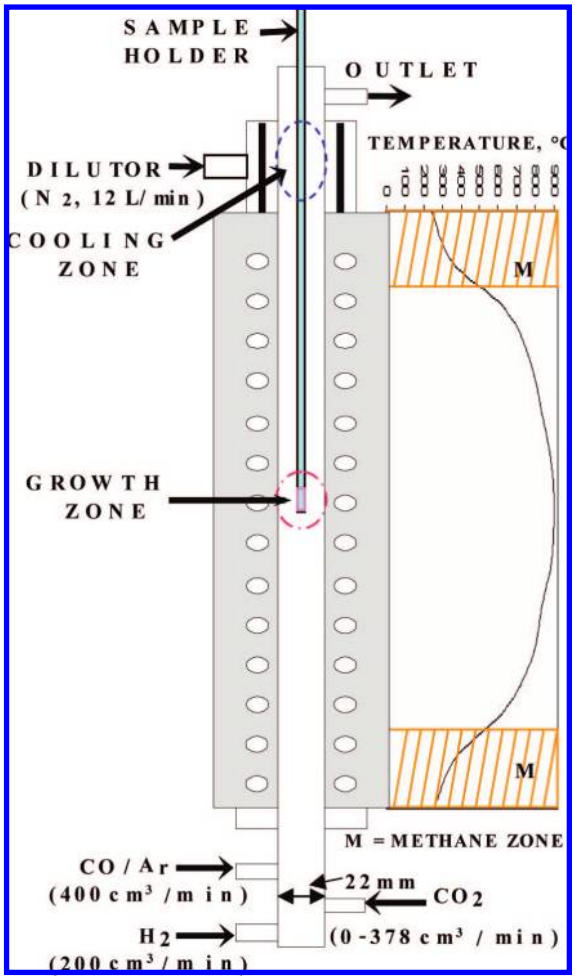

Figure 1. Schematic representation of the CVD reactor along with a temperature profile at 900 °C.

material was attached to a stainless steel rod and then inserted into the middle of the reactor. A thermocouple was placed inside the rod to monitor the temperature of the CNT growth. Then, a H_2 flow (200 cm^3/min) was introduced into the reactor. After 5 min, Ar flow was replaced by CO with the same flow rate. After 30 min of growth time, H_2 and CO flows were replaced by Ar, and the rod was pulled to the dilutor, which was used for cooling the substrate to a temperature below 100 °C. The dilutor was a porous tube, through which a 12 L/min room temperature N_2 flow was introduced. A certain concentration of CO_2 was constantly fed into the reactor for the entire duration of the experiments. The reduction and growth periods were kept constant for most of the experiments unless otherwise specified. The experiments were carried out under atmospheric pressure in a temperature range from 590 to 1120 °C.

Scanning electron microscopy (SEM, Leo Gemini DSM982) and field emission transmission electron microscopy (TEM, Philips CM200 FEG) were used for characterizing CNTs. For TEM observation, nanotubes were directly grown on SiO_2/SiO-Ni TEM grids (SPI, USA). The outlet gas phase composition was analyzed online by a Gasmet Fourier-transform infrared (FT-IR) spectrometer.

2.2. Experimental Results. In order to investigate the effect of the Fe amount on CNT morphology, the sputtering time of the catalyst material was varied from 5 to 20 s. For the current examination, reactor temperature was fixed at 900 °C. The mole fraction of the introduced CO_2 was kept at 0.7%, which corresponded to the flow rate of 4 cm^3/min. At the lowest

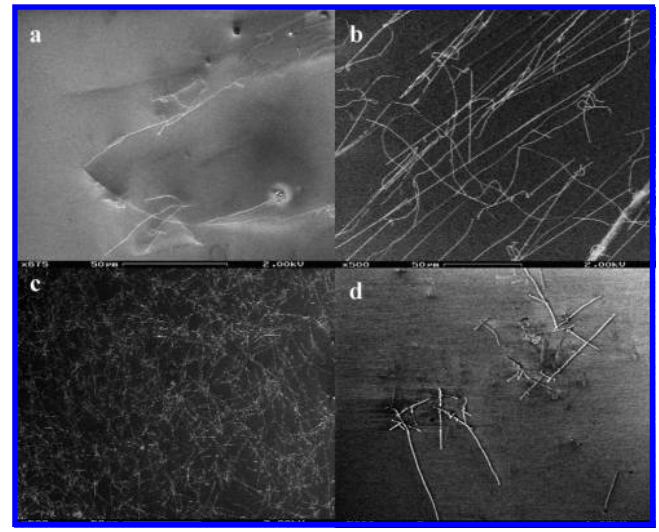

Figure 2. SEM images showing the effect of sputtering time on the density of CNTs at 900 °C and CO_2 concentration of 0.7%: (a) 5, (b) 10, (c) 15, and (d) 20 s.

sputtering duration of 5 s, very few CNTs were found on the substrate (Figure 2a). Increasing the sputtering time to 10 s resulted in an increase in the density of CNTs (Figure 2b). Maximum CNT density was found at a sputtering time of 15 s (Figure 2c). When the sputtering time was increased further, the density of CNTs decreased. This can be likely explained by excessive aggregation of catalyst particles, which were not favorable for CNT nucleation and growth. In order to avoid this at higher temperatures, when the mobility or collision rate of catalyst particles on the substrate surface is significantly enhanced, we reduced the sputtering time. For instance, at 970 and 1070 °C, the growth of CNTs was found to be optimum with sputtering times of 11 and 7 s, respectively. For all further experiments at 900 °C and below, a sputtering time of 15 s was used unless otherwise specified.

The effect of CO_2 concentration on CNT density was examined at different temperatures. It was found that CNT growth could take place without added CO_2. However, the density of the produced CNTs was significantly less compared to that in optimum synthesis conditions, i.e., when a certain CO_2 concentration was added. Figure 3 shows the variation in product morphology at 900 °C. Increasing the CO_2 mole fraction to 1.32% (8 cm^3/min) resulted in a regular increase in CNT density. However, further increase in CO_2 concentration led to the decrease in the amount of synthesized CNTs. At a mole fraction of 2.75%, no CNTs were found on the substrate. Therefore, at the highest CNT density, the CO_2 concentration was 1.32% at 900 °C. For successful CNT synthesis at higher temperatures of 970, 1070, and 1120 °C, the CO_2 mole fractions were found to decrease to 0.25, 0.083, and 0.075%, respectively. At lower temperatures from 740 to 590 °C, the optimum concentration increased and varied from 2.0 to 38.7% respectively.

TEM observation of CNTs produced at optimum CO_2 concentrations at different conditions revealed an interesting feature: increasing the temperature in the reactor resulted in an increase in the number of CNT walls (Table 1). Only single-walled CNTs were synthesized at 590 °C (Figure 4a). Twenty nanotubes were observed at this temperature. TEM characterization of the samples produced at 740 °C revealed predominant single-walled CNT formation. An observation of 25 tubes found that only two tubes were double-walled. Increasing the temperature to 900 °C led to the predominant formation of double-

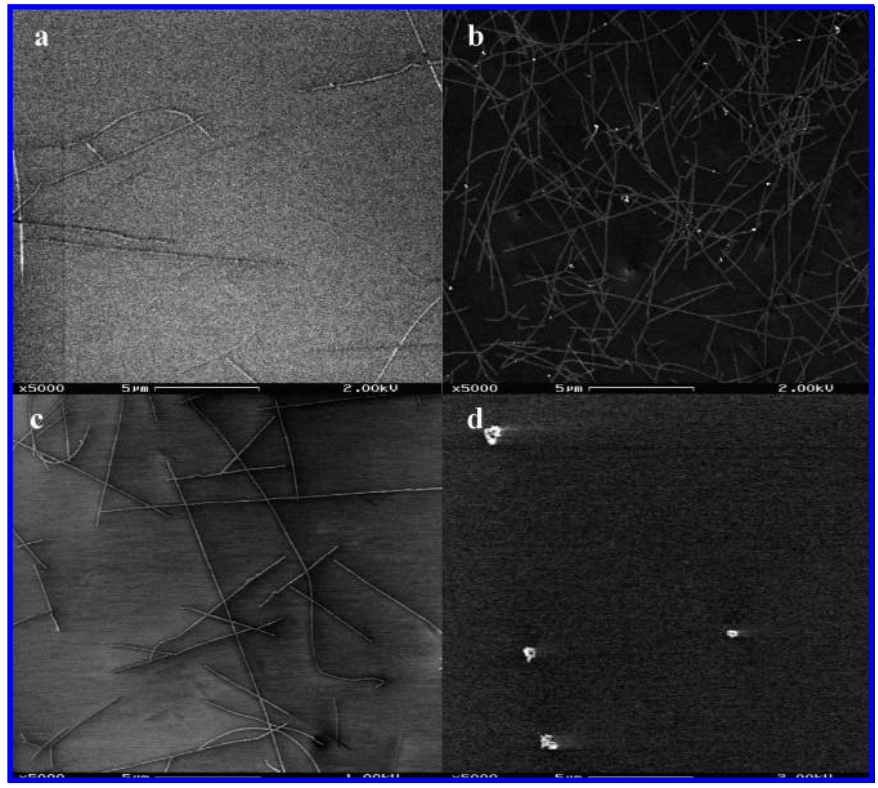

Figure 3. SEM images showing the effect of the CO_2 mole fraction on CNT growth at 900 °C and sputtering time of 15 s: (a) 0, (b) 1.32, (c) 2.12, and (d) 2.75%.

TABLE 1: Variation in the Number of Walls, Diameter, and Length of CNTs Produced under Different Conditions

temperature (°C)	CO_2 concentration (%)	product (number of walls)	nanotube diameter (nm)	variation in length (μm)
590	38.7	1	2.1–2.4	>2
740	2.00	1,2	1.4–2.5	0.5–25
900	1.32	2,1	3.6–8.4	2–100
970	0.25	3,2	3.7–7.3	2–200
1070	0.083	4,3,2	4.5–12	>350

walled CNTs, and only 5 of 32 nanotubes were single-walled. A typical TEM image of a double-walled CNT is shown in Figure 4b. At 970 °C, 10 triple-walled, 6 double-walled, 3 quadruple-walled, and 1 single-walled CNTs were found. A typical TEM image of a triple-walled CNT is shown in Figure 4c. At 1070 °C, mainly quadruple-walled CNTs were found (Figure 4d); however, a few CNTs with three and five walls were also detected under this condition.

It is worth noting that the diameters and lengths of CNTs also follow the similar temperature trend: the higher the temperature, the larger and longer the tubes. The variation in CNT diameter from 1.4 to 12 nm can be seen in Table 1. Short tubes of about 500 nm were synthesized at low temperatures, while at high temperatures the length of the tube exceeded 350 μm. Another important feature is that the ratio between the diameters of catalyst particles and CNTs was around one. In some cases, especially for large CNTs, the tube diameter exceeded the size of the catalyst particles (Figure 5). Incidentally, while characterizing the CNTs in TEM, we found that many catalyst particles were completely detached or indirectly attached to (not embedded inside) CNTs (Figure 5). These findings will be discussed in the next section of the paper.

In order to investigate the size of the catalyst particles on the substrates obtained at different iron deposition time and temperatures, we prepared a few TEM grids treated in an Ar atmosphere at 590 and 900 °C for 30 min with sputtering times of 7 and 15 s. As can be seen in Figure 6, quite homogeneous

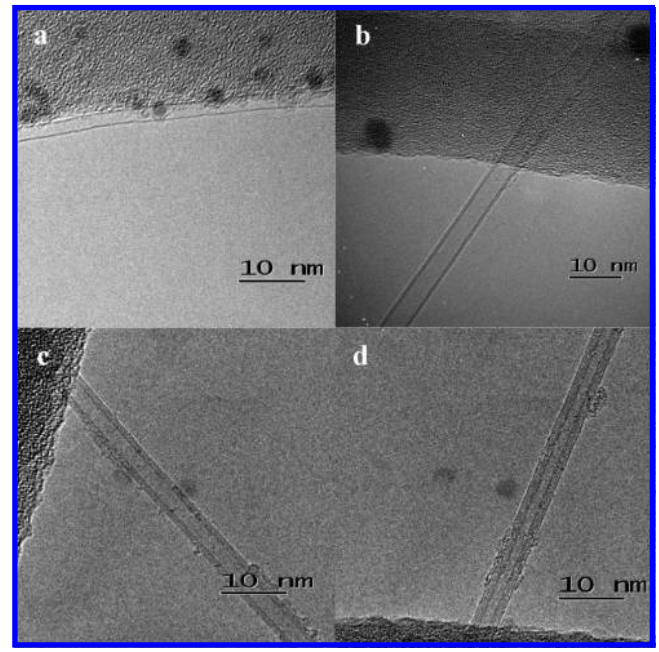

Figure 4. TEM images of typical products synthesized at different temperatures: (a) single-walled CNT at 590 °C, (b) double-walled CNT at 900 °C, (c) triple-walled CNT at 970 °C, and (d) quadruple-walled CNT at 1070 °C.

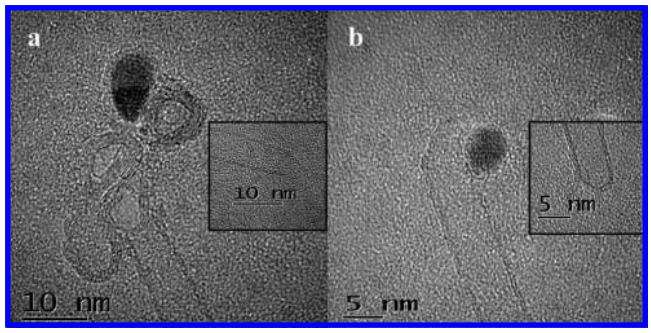

Figure 5. TEM images of CNTs together with particles that catalyzed their growth. Inset images show the other ends of the tubes.

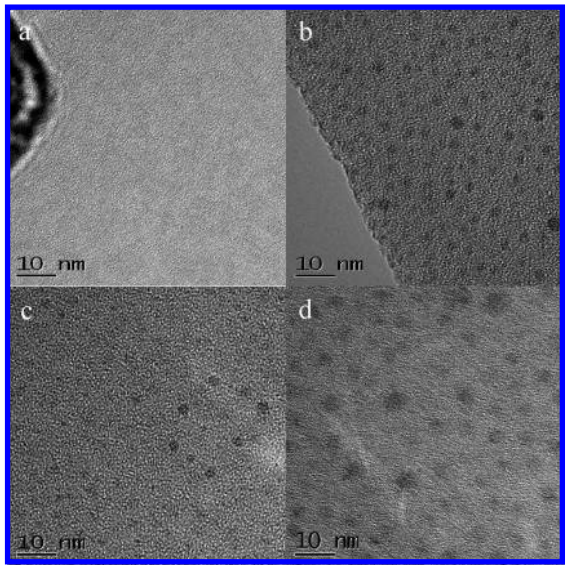

Figure 6. TEM images of catalyst particles treated in an Ar atmosphere: (a) 15 s sputtering time and no heat treatment, (b) 15 s sputtering time and treated at 590 °C, (c) 7 s sputtering time and treated at 900 °C, and (d) 15 s sputtering time and treated at 900 °C.

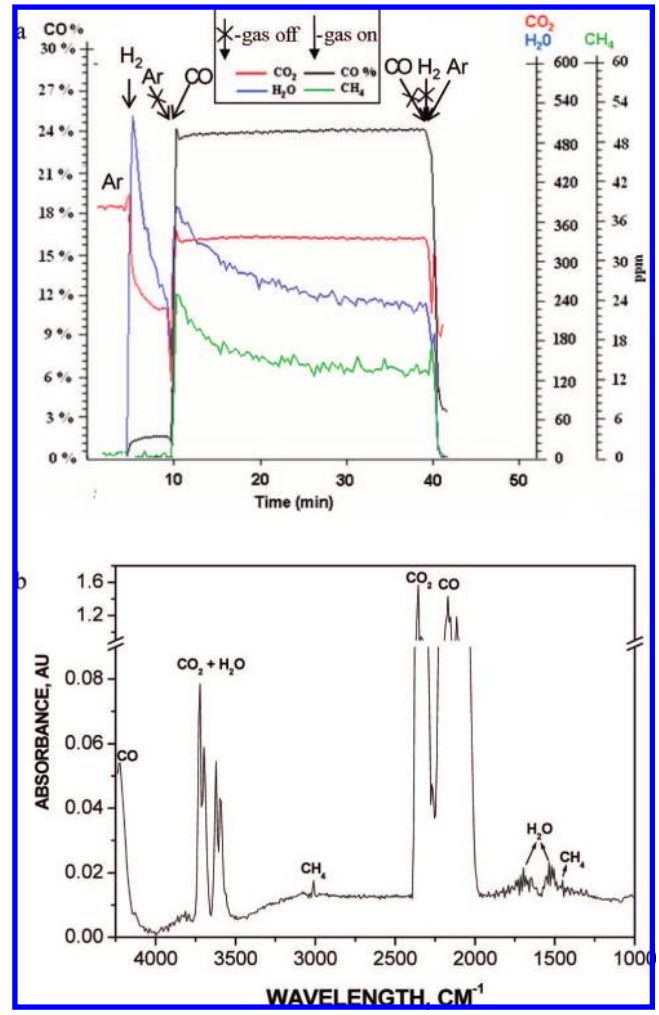

Figure 7. Results of FT-IR measurements from the reactor at 900 °C: (a) time dependence of gaseous components during the process of CNT synthesis and (b) IR spectrum revealing the formation of methane.

deposition was obtained on the nonthermally treated substrate. At a fixed sputtering time, the particle size increased from about 2 to 3.5 nm with an increase in temperature from 590 to 900 °C, respectively. Also seen in Figure 6, the size of the catalyst particles at different temperatures can be controlled by the sputtering time. A sample with a 7 s sputtering time treated at 900 °C and a sample with a 15 s sputtering time treated at 590 °C resulted in very similar sizes. Therefore, in order to examine the effect of the catalyst particle diameter on the number of walls we decreased the sputtering time at 900 and 970 °C to 6 and 7 s, respectively. However, this did not significantly affect the number of walls. For instance, CNTs produced at 900 °C were mainly double-walled, however, with smaller diameters of about 2 nm. Decreasing the sputtering time to 7 s at 970 °C allowed us to produce triple-walled and double-walled CNTs with diameters of 3.3−7.2 nm.

It is worth noting that CO disproportionation is an exothermic reaction and restricted at high temperatures.[30] In situ samplings performed in two different CNT aerosol reactors[30,31] based on CO disproportionation reactions detected that the growth of CNTs stopped at temperatures of about 900 °C. However, CNTs were grown at 1120 °C in the present system. This gave us evidence for suggesting the existence of another carbon source in addition to carbon monoxide. In order to examine this hypothesis we performed online FT-IR measurements of the gaseous products coming from the reactor at 900 °C during the CNT synthesis (Figure 7). When H_2 was added to the Ar and CO_2 flows, this led to the water−gas shift reaction[32] and the formation of CO and H_2O. After introduction of CO into the reactor, 13−25 ppm of CH_4 was detected. This amount of methane, taking into account a 30 min growth duration, might be sufficient for CNT growth. When CO and H_2 were switched to Ar, the CH_4 disappeared from the gaseous products.

The formation of methane upstream of the reactor can affect the CNT structure as well as the wall number alteration with the temperature increase due to the gradual change of the reactive carbon precursor in the reactor from CO to CH_4. This was examined by introducing additional CH_4 amounts (715 and 3560 ppm) into the reactor at 900 and 970 °C. However, no significant effect on the morphology and the number of walls of CNTs was observed. Additional experiments carried out with a mixture of CH_4 and H_2, i.e., without CO, did not lead to the formation of CNTs. Therefore, methane can be ruled out as being the carbon source by determining the structure and morphology of CNTs grown at high temperatures.

3. Discussion

Let us first discuss the most important chemical reactions, which might happen in the reactor. Here we apply a thermodynamic approach in order to explain the possibility of the reaction occurrences and show their temperature tendencies. The

thermodynamic calculations were carried out using the F*A*C*T software.[33] The values of enthalpies for different reactions are given for a temperature of 900 °C. For the calculations, we used the thermodynamic data for graphitic carbon C and α-Fe.

The main source of carbon for CNT growth was the Boudouard reaction (CO disproportionation):

$$CO_{(g)} + CO_{(g)} \leftrightarrow C + CO_{2(g)}, \Delta H = -169 \text{ kJ/mol} \quad (1)$$

Because H_2 was present in the reactor, another reaction, CO hydrogenation, leading to the carbon release could occur:

$$CO_{(g)} + H_{2(g)} \leftrightarrow C + H_2O_{(g)}, \Delta H = -136 \text{ kJ/mol} \quad (2)$$

Applying the rule of summation for reactions 1 and 2, one can get a water−gas shift reaction

$$CO_{(g)} + H_2O_{(g)} \leftrightarrow H_{2(g)} + CO_{2(g)}, \Delta H = -33 \text{ kJ/mol} \quad (3)$$

determining the relative concentration of the gaseous species. Reactions 1 and 2 have very similar thermodynamic behavior.[30] At low temperatures, these reactions are shifted toward the formation of carbon. The thermodynamic equilibrium ($\Delta G = 0$) is observed at a temperature of approximately 700 °C (Figure 8a). Kinetic investigations of reaction 1 show appreciable reaction rates in the temperature interval from 470 to 820 °C.[30] At higher temperatures, the inverse reactions prevail. At temperatures lower than 325 °C, this reaction is limited kinetically, and at high temperatures, it is thermodynamically prohibited. However, reaction 1 (as well as reaction 2) can occur at 900 °C even though $\Delta G_{900} > 0$ because the equilibrium concentration of CO_2 at this temperature is about 2.7%. It was experimentally shown in CVD[34] and aerosol[28,30,35] reactors that CNTs could be grown from CO in the temperature range of 600−928 °C.

It is worth noting that the experimentally optimized concentrations of CO_2 needed for successful CNT synthesis were slightly less than the equilibrium values (Figure 8a). If the concentration of the introduced CO_2 was higher than the equilibrium value, then the equilibrium of reaction 1 would be shifted to the left, and CO disproportionation would not occur. Thus, the optimized CO_2 concentration values are in a good agreement with the thermodynamic approach applied in this work (Figure 8a).

As was shown, CO_2 played a very important role in the variation in the product morphology. The absence of introduced CO_2 as well as its excessive presence reduces the density of the CNTs, which implies disadvantageous conditions for the activation of catalyst particles. Most likely (i) the etching effect, i.e., removing excess catalyst and/or "poisoning" carbon, and (ii) the prevention of catalyst particle passivation or the activation of catalyst particles can be attributed to CO_2 according to[36]

$$Fe_3C + CO_{2(g)} \leftrightarrow 3Fe + 2CO_{(g)}, \Delta H = 146 \text{ kJ/mol} \quad (4)$$

because cementite is known to be an inactive phase for fiber and CNT formation.[37,38] Reaction 4 is thermodynamically favorable ($\Delta G > 0$) at temperatures higher than 685 °C, whereas at lower temperatures the inverse reaction of cementite formation occurs. Also, one should mention the possibility of cementite formation because of the direct reaction between carbon and iron:

$$3Fe + C \leftrightarrow Fe_3C, \Delta H = 12 \text{ kJ/mol} \quad (5)$$

FT-IR measurements revealed formation of CH_4 in the reactor. The formation of CH_4 can be attributed to reactions of H_2 with CO

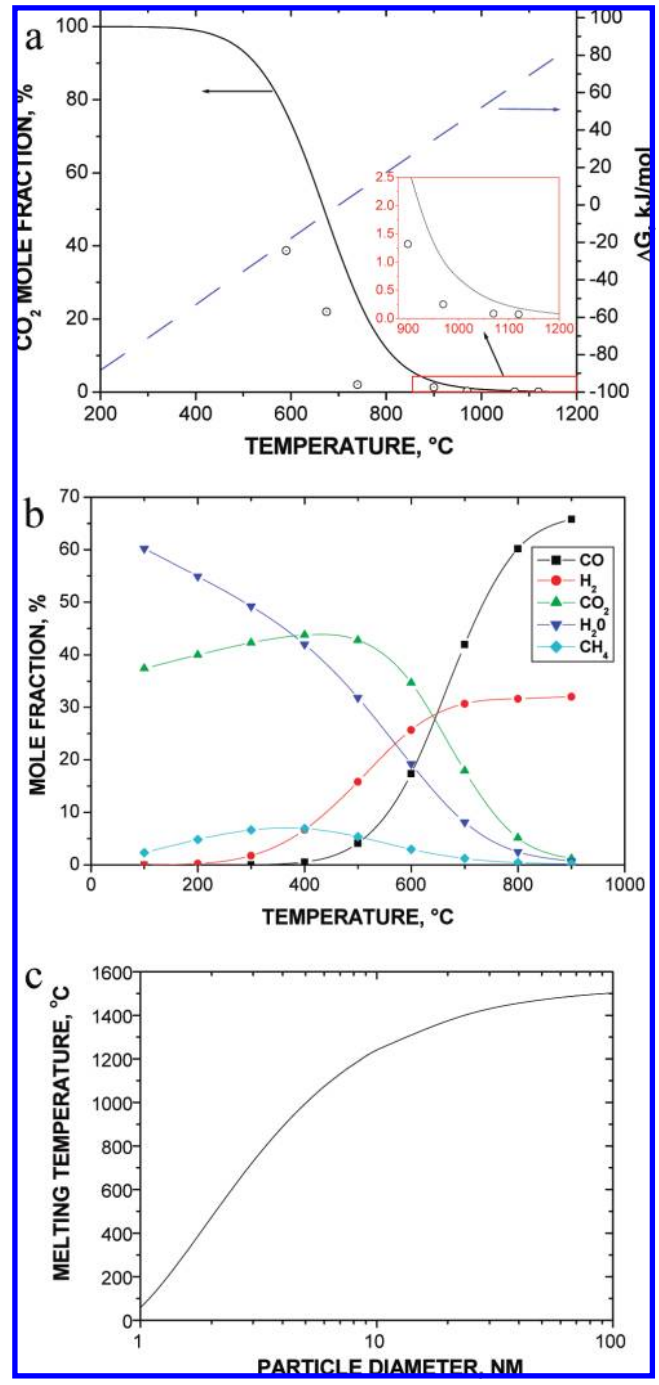

Figure 8. Results of thermodynamic calculations: (a) CO disproportionation with temperature dependence of the Gibbs free energy and equilibrium CO_2 mole fraction, together with experimentally optimized concentrations for CNT growth (open dots); (b) gaseous product after mixing 2 mol of CO, 1 mol of H_2, and CO_2 (1.3%). (c) Effect of particle size on melting temperature of the Fe particles.

$$3H_{2(g)} + CO_{(g)} \leftrightarrow CH_{4(g)} + H_2O_{(g)}, \Delta H = -227 \text{ kJ/mol} \quad (6)$$

or with carbon

$$2H_{2(g)} + C_{(s)} \leftrightarrow CH_{4(g)}, \Delta H = -91 \text{ kJ/mol} \quad (7)$$

In order to examine the possibility of methane formation, we carried out thermodynamic calculations determining the product, which could be formed at different temperatures in the reactor. When we calculated a mixture of 2 mol of CO and 1 mol of H_2, corresponding to the experimental conditions (400 cm^3/min CO and 200 cm^3/min H_2), the maximum methane concentration

was found to be around 370 °C, which is in good agreement with the literature.[36−40] There are two zones in the reactor with this temperature, the upper and lower part of the reactor (Figure 1). Because methane formation requires the presence of a catalyst, CH_4 was most likely formed on the reactor walls. The alumina ceramic tube used for the experiments contained SiO_2 (0.25%), Ca (0.02%), Fe (0.02%), and Cd (0.09%) impurities. The amount of ceramic impurities capable of catalyzing the methanation process, taking into account a very high surface area of the ceramic materials, can be sufficient for the formation of a 10 ppm level of CH_4.[39−43] In order to confirm that the methane was formed on the reactor walls, we replaced the ceramic tube with a quartz tube. FT-IR measurements detected no methane formation in the quartz tube reactor.

Now let us discuss the most intriguing result of this paper: the incremental variation in the number of CNT walls with increasing temperature. As was shown in the Experimental Section, this behavior cannot be explained by a gradual change of the reactive carbon precursor in the reactor from CO to CH_4 at high temperatures. Neither is the increase in catalyst particle size alone responsible for the formation of thin multiwalled CNTs because a decrease in sputtering time, i.e., decreasing the catalyst particle size, did not lead to a significant change in the number of walls of the produced CNTs, although the CNT diameters were reduced.

It is known that the properties of the small particles significantly differ from those of the bulk material. The melting temperature T_m for a given particle of radius r can be estimated on the basis of the Kelvin equation

$$T_m = T_o \exp\left(-\frac{2\sigma_{sl}V}{r\Delta H_{fus}}\right) \quad (8)$$

where T_o is the bulk melting temperature (1535 °C); ΔH_{fus} is the latent heat of fusion (13.8 kJ/mol); V is the volume of a metal molecule, which can be calculated from the density (7.87×10^3 kg/m^3); and σ_{sl} is the surface tension between liquid and solid (0.86 J/m^2). The results of the calculations are plotted in Figure 8c. As one can see, catalyst particles 4−5 nm in diameter are expected to be in a liquid state at temperatures above 890−1000 °C. At lower temperatures, catalyst particles are in the solid phase and as a result produce single-walled CNTs, which is expected from the literature.[44,45] At high temperatures, the catalyst particles are in the liquid state and promote the formation of CNTs with larger numbers of walls. These follow from the diffusion model[46−48] and can be explained by an increase in carbon solubility[49] and diffusivity[30] in liquid iron. These properties are significantly enhanced with temperature, which also leads to an increase in the length and number of CNT walls. An increase in temperature also increases the diffusivity of carbon atoms on the surface of both iron particles and CNTs.

As mentioned before, the analysis of catalyst particles and CNT dimensions under different conditions indicated a good correlation. The ratio between the diameters of the particles and CNTs was found to be close to one and less in some cases. This contradicts our previously reported results[50] obtained also in the Fe-CO system; however, in an aerosol reactor, this ratio was measured to be 1.5−1.6. We believe that the discrepancy can be explained by the presence of the substrate and its effect on the mechanism of CNT growth as well as on TEM observation of CNTs. The latter can be seen in Figure 5b, where the CNT diameter is larger than the catalyst particle that initiated its growth. Apparently, this artifact can be explained by CNT deformation (flattening) due to the interaction with the substrate, which is known to happen with CNTs larger than 2.7 nm in diameter.[51]

As reported in the previous section, many catalyst particles were completely detached or indirectly attached to (not embedded inside) CNTs (Figure 7). This abnormal connection between catalyst particles and CNTs can be explained by fast quenching of the CNT growth, namely by the rapid cooling of CNTs in the dilutor and the sudden release of dissolved carbon from the catalyst particle. This could be a quite interesting approach to detach catalyst particles from CNTs and might allow synthesis of catalyst-free nanotubes.

4. Conclusion

We have synthesized CNTs in a substrate CVD reactor using CO and Fe as carbon and catalyst sources, respectively. Depending on the synthesis conditions, CNTs were from 1.4 to 12 nm in diameter. Increasing the temperature resulted in an increase in the CNT length from 0.5 to 350 μm. We have demonstrated a variation in the number of CNT walls from one to four by changing the synthesis temperature from 590 to 1070 °C, together with changing the CO_2 concentration. These incremental variations in the number of CNT walls and CNT lengths with temperature can be explained by an enhancement of carbon solubility and diffusivity.

The effect of sputtering time and the amount of CO_2 on the density of the produced CNTs was studied. The crucial role of CO_2 in the activation of catalyst particles and, as a result, in the control of the CNT density was demonstrated. Etching the amorphous carbon from the catalyst particles and the prevention of the formation of the cementite phase we have attributed to CO_2.

Acknowledgment. We thank Dr. Paula Queipo for performing the preliminary synthesis of CNTs in a quartz tube reactor. This work was supported by the Finnish National Graduate School in Nanoscience (NGS-NANO) and the Academy of Finland.

References and Notes

(1) Iijima, S. *Nature* **1991**, *354*, 56.
(2) Dresselhaus, M. S.; Dresselhaus, G.; Eklund, P. C. *Science of Fullerenes and Carbon Nanotubes*; Academic Press: San Diego, 1996.
(3) Reich, S.; Thomsen, C.; Maultzsch, J. *Carbon Nanotubes, Basic Concepts and Physical Properties*; Wiley-VCH Verlag GmbH & Co.: Weinheim, Germany, 2004.
(4) Bockrath, M.; Cobden, D. H.; McEuen, P. L.; Chopra, N. G.; Zettl, A.; Thess, A.; Smalley, R. E. *Science* **1997**, *275*, 1922.
(5) Tans, S. J.; Devoret, M. H.; Dai, H.; Thess, A.; Smalley, R. E.; Geerligs, L. J.; Dekker, C. *Nature* **1997**, *386*, 474.
(6) Chico, L.; Crespi, V. H.; Benedict, L. X.; Louie, S. G.; Cohen, M. L. *Phys. Rev. Lett.* **1996**, *76*, 971.
(7) Zhaoa, J.; Xieb, R. H. *J. Nanosci. Nanotechnol.* **2003**, *3*, 459.
(8) Robertson, J. *Mater. Today* **2004**, *7*, 46.
(9) Iijima, S.; Ichihashi, T. *Nature* **1993**, *363*, 603.
(10) Bethune, D. S.; Kiang, C. H.; De Vries, M. S.; Gorman, G.; Savoy, R.; Vazquez, J.; Beyers, R. *Nature* **1993**, *363*, 605.
(11) Guo, T.; Nikolaev, P.; Thess, A.; Colbert, D. T.; Smalley, R. E. *Chem. Phys. Lett.* **1995**, *243*, 49.
(12) Zhou, Z.; Ci, L.; Chen, X.; Tang, D.; Yan, X.; Liu, D.; Liang, Y.; Yuan, H.; Zhou, W.; Wang, G.; Xie, S. *Carbon* **2003**, *41*, 337.
(13) Bladh, K.; Falk, L. K. L.; Rohmund, F. *Appl. Phys. A: Mater. Sci. Process.* **2000**, *70*, 317.
(14) Nasibulin, A. G.; Moisala, A.; Brown, D. P.; Jiang, H.; Kauppinen, E. I. *Chem. Phys. Lett.* **2005**, *402*, 227.
(15) Dai, H.; Rinzler, A. G.; Nikolaev, P.; Thess, A.; Colbert, D. T.; Smalley, R. E. *Chem. Phys. Lett.* **1996**, *260*, 471.
(16) Bachilo, S. M.; Balzano, L.; Herrera, J. E.; Pompeo, F.; Resasco, D. E.; Weisman, R. B. *J. Am. Chem. Soc.* **2003**, *125*, 11186.
(17) Miyauchi, Y.; Chiashi, S.; Murakami, Y.; Hayashida, Y.; Maruyama, S. *Chem. Phys. Lett.* **2004**, *387*, 198.

(18) Moshkalev, S. A.; Verissimo, C. *J. Appl. Phys.* **2007**, *102*, 044303.
(19) Gavrilov, V. Yu.; Grishin, D. A.; Jiang, H.; Digurov, N. G.; Nasibulin, A. G.; Kauppinen, E. I. *Russ. J. Phys. Chem.* **2007**, *81*, 1502.
(20) Valles, C.; Perez-Mendoza, M.; Martínez, M. T.; Maser, W. K.; Benito, A. M. *Diamond Relat. Mater.* **2007**, *16*, 1087.
(21) Harutyunyan, A. R.; Mora, E.; Tokune, T.; Bolton, K.; Rosen, A.; Jiang, A.; Awasthi, N.; Curtarolo, S. *Appl. Phys. Lett.* **2007**, *90*, 163120.
(22) Liu, J.; Fan, S.; Dai, H. *MRS Bull.* **2004**, *29*, 244.
(23) Hata, K.; Futaba, D. N.; Minuzo, K.; Namai, T.; Yumura, M.; Ijima, S. *Science* **2004**, *306*, 1362.
(24) Takagi, D.; Homma, Y.; Hibino, H.; Suzuki, S.; Kobayashi, Y. *Nano Lett.* **2006**, *6*, 2642.
(25) Oncel, C.; Yurum, Y. *Fullerenes, Nanotububes, Carbon Nanostruct.* **2006**, *14*, 17.
(26) Panchakarla, L. S.; Govindaraj, A.; Rao, C. N. R. *ACS Nano* **2007**, *1*, 494.
(27) Qiu, H.; Shi, Z.; Gu, Z.; Qiu, J. *Chem. Commun.* **2007**, 1092.
(28) Moisala, A.; Nasibulin, A. G.; Brown, D. P.; Jiang, H.; Khriachtchev, L.; Kauppinen, E. I. *Chem. Eng. Sci.* **2006**, *61*, 4393.
(29) Queipo, P.; Nasibulin, A. G.; Gonzalez, D.; Tapper, U.; Jiang, H.; Tsuneta, T. H.; Grigoras, K.; Duenas, J. A.; Kauppinen, E. I. *Carbon* **2006**, *44*, 1581.
(30) Nasibulin, A. G.; Queipo, P.; Shandakov, S. D.; Brown, D. P.; Jiang, H.; Pikhitsa, P. V.; Tolochko, O. V.; Kauppinen, E. I. *J. Nanosci. Nanotechnol.* **2006**, *6*, 1233.
(31) Nasibulin, A. G.; Shandakov, S. D.; Anisimov, A. S.; Brown, D. P.; Jiang, H.; Pikhitsa, P. V.; Kauppinen, E. I. Role of Catalyst Particles During CNT Growth. *Book of Abstracts*, NT'7 Eighth International Conference on the Science and Application and Nanotubes, Ouro Preto, Brazil, June 24−29, 2007; p 43.
(32) Nasibulin, A. G.; Brown, D. P.; Queipo, P.; Gonzalez, D.; Jiang, H.; Kauppinen, E. I. *Chem. Phys. Lett.* **2006**, *417*, 179.
(33) Bale, C. W.; Chartrand, P.; Degterov, S. A.; Eriksson, G.; Hack, K.; Mahfoud, R. B.; Melancon, J.; Pelton, A. D.; Petersen, S. *CALPHAD: Comput. Coupling Phase Diagrams Thermochem.* **2002**, *26*, 189.
(34) Queipo, P.; Nasibulin, A. G.; Jiang, H.; Gonzalez, D.; Kauppinen, E. I. *Chem. Vap. Deposition* **2006**, *12*, 364.
(35) Kulikov, I. S. *Thermodinamika Karbidov i Nitridov: Spravochnik. (Thermodynamics of Carbides and Nitrides: A Handbook)*; Metallurgija: Cheljabinsk, 1988; in Russian.
(36) Audier, M.; Coulon, M.; Bonnetain, L. *Carbon* **1983**, *21*, 93.
(37) Baker, R. T. K.; Alonzo, J. R.; Dumesic, J. A.; Yates, D. J. C. *J. Catal.* **1982**, *77*, 74.
(38) Hernadi, K.; Fonseca, A.; Nagy, J. B.; Fudala, A.; Bernaerts, D.; Kiricsi, I. *Appl. Catal., A* **2002**, *228*, 103.
(39) Lo, J. M. H.; Ziegler, T. *J. Phys. Chem. C* **2007**, *111*, 11012.
(40) Sehested, J.; Larsen, K. E.; Kustov, A. L.; Frey, A. M.; Johannessen, T.; Bligaard, T.; Andersson, M. P.; Norskov, J. K.; Christensen, C. H. *Top. Catal.* **2007**, *45*, 9.
(41) Tahir, A. H. K. Methanation-Bimetallic Catalysts. Ph.D. Thesis, University of the Punjab, Pakistan, 1992.
(42) Weisang, E.; Engelhard, P. A. *Chim. Ind. Genie Chim.* **1970**, *103*, 287.
(43) Choudhury, M. B. I.; Ahmed, S.; Shalabi, M. A.; Inui, T. *Appl. Catal., A* **2006**, *314*, 47.
(44) Maruyama, S.; Kojima, R.; Miyauchi, Y.; Chiashi, S.; Kohno, M. *Chem. Phys. Lett.* **2002**, *360*, 229.
(45) Bachilo, S. M.; Balzano, L.; Herrera, J. E.; Pompeo, F.; Resasco, D. E.; Weisman, R. B. *J. Am. Chem. Soc.* **2003**, *125*, 11186.
(46) Baker, R. T. K.; Barber, M. A.; Barber, P. S.; Harris, P. S.; Feates, F. S.; Waite, R. J. *J. Catal.* **1972**, *26*, 51.
(47) Baker, R. T. K.; Harris, P. S.; Henderson, F.; Thomas, R. B. *Carbon* **1975**, *13*, 17.
(48) Rodriguez, N. M. *J. Mater. Res.* **1993**, *8*, 3233.
(49) Massalski, T. B. *Binary Alloy Phase Diagrams*; ASM International: Materials Park, OH, 1996.
(50) Nasibulin, A. G.; Pikhitsa, P. V.; Jiang, H.; Kauppinen, E. I. *Carbon* **2005**, *43*, 2251.
(51) Queipo, P.; Nasibulin, A. G.; Shandakov, S. D.; Jiang, H.; Gonzalez, D.; Kauppinen, E. I. CVD Synthesis and Radial Deformations of Large Diameter Single-Walled CNTs. *Curr. Appl. Phys.* **2009**, *9*, 301.

JP808316P